Experimental Investigation of Heat Transfer Performance of Corrugated Tube with Spring Tape Inserts

Suvanjan Bhattacharyya[a], Ali Cemal Benim[b,c*], Himadri Chattopadhyay[d],

Arnab Banerjee[e],

[a]Department of Mechanical and Aeronautical Engineering, University of Pretoria, Pretoria 0002, South Africa

[b]Center of Flow Simulation (CFS), Department of Mechanical and Process Engineering, Duesseldorf University of Applied Sciences, Muensterstr. 156, D-40476, Duesseldorf, Germany

[c]Institute of Thermal Power Engineering, Department of Mechanical Engineering, Cracow University of Technology, Al. Jana Pawła II 37, 31-864 Cracow, Poland

[d]Mechanical Engineering Department, Jadavpur University, Kolkata – 700 032, West Bengal. India

[e]Mechanical Engineering Department, MCKV Institute of Engineering, Liluah, Howrah – 711204, West Bengal. India

*Corresponding Author: Prof. Dr. A. C. Benim, Center of Flow Simulation (CFS), Department of Mechanical and Process Engineering, Duesseldorf University of Applied Sciences, Muensterstr. 156, D-40476 Duesseldorf, Germany,

E-mail: alicemal@prof-benim.com

ABSTRACT

Turbulent forced convection in a corrugated tube with spring tape is investigated experimentally, for Reynolds numbers from 10,000 to 50,000. The working fluid is air. Experiments are performed for different pitch and spring ratios. Results show that Nusselt numbers can be increased considerably, depending on pitch and spring ratios. An overall assessment, considering the friction losses, is achieved using the thermo-hydraulic performance parameter. The latter is observed to take values larger than unity for all cases, were quite high values around 2.8 occur for cases with smallest pitch and spring ratios. Predictive Nusselt number and friction factor correlations are proposed.

Keywords: Heat transfer enhancement, Corrugated tube, Spring tape

1. Introduction

Heat transfer enhancement is a focus with extensive concern to researchers and engineers to save power requirement and expenditure, in a wide range of technical applications [1]. Passive and active heat transfer augmentation methods in channels of such devices have consequently been a focal point of intensive experimental and computational research [2-12]. Swirling devices have been among the leading members of heat transfer enrichment techniques [12]. As the swirl increases, the near-wall velocity and, consequently, the wall shear stress increase in magnitude, enhancing the convective transport ability of the fluid, with higher demands on the computational modelling [13], however, due to the increased anisotropy of the turbulence structure.

Researches were also performed on other passive improvement methods, like channels with artificial roughness and inlet disturbances. Delta-wing/winglet type vortex generators on heat transfer surfaces have been among the intensively investigated passive heat transfer augmentation methods [14-18], which interrupt the boundary layer and enhance turbulence by generating stream wise longitudinal vortices. Fiebig et al. [19] assessed the consequence of delta-winglet vortex generators on heat exchange and flow stream characteristics of a fin-channel heat exchanger with flat and round channels. The consequences furnished that the strong longitudinal vortices generated by the delta-winglet vortex generators increase both the heat exchange and pressure penalty of the fin-channel heat exchanger. The results also showed that the rate of heat exchange was higher by 20% while the friction penalty quadrupled for the fin-round channel heat exchanger compared with those for the fin-flat channel heat exchanger. Coiled wire inserts have been used, where the tube boundary layer is interrupted and turbulated as the near-wall flow trips over the wire [20,21], or around it, if the wire is slightly separated from the wall [22]. As the twisted tape (also called as screw tape) inserts have been quite intensively analyzed as a heat transfer enhancement technique, auxiliary measures such as

louvres, perforations, and surface roughness on the tape, as well as eccentricity between the tape and the tube have also been applied in combination to achieve a performance improvement [23-29].

Wongcharee and Eiamsa-ard [30] studied the effect of CuO-water nanofluid and twisted tape with alternate axis (TA) on thermo-hydraulic characteristics. The experimental data furnished that the use of TA resulted in heat transfer enrichment up to 12.8 times of that of water in the plain channel. Eiamsa-ard et al. [31] conducted experiments on twisted tape having twisting ratio of 6 to 8 for full length tape and free space ratio 1, 2 and 3 for evenly spaced twisted tape insert. Results indicated that the coefficient of heat exchange rises with drop off in twist ratio and space ratio. Eiamsa-ard et al. [32] investigated short length twisted tape inclusions. They engaged twisted tape with constant twist ratio and different length ratio. Short length inserts generated powerful swirl at channel entry while the full length tape produced strong swirl flow over the entire length. Sarada et al. [33] observed that width of twisted tape considerably affects the rate of heat exchange. It was found that heat transfer enriches as per the increase in the width of insert. Piriyarungrod et al. [34] found that taper was not an effective measure to further increase the heat transfer using twisted tape inclusions. Esmaeilzadeh et al. [35] assessed the consequence of thickness of twisted tape with nanofluid by showing that the raise in thickness increases the heat transfer rate, the friction factor and the thermo-hydraulic performance. Eiamsa-ard and Promvonge [36] extensively investigated the performance of subsequently clockwise and counterclockwise twisted tape inclusions. They included tapes in assessments having twist ratios of 3, 4 and 5 each with three twist angles 30°, 60° and 90°. Results indicated that the heat transfer rate and thermo-hydraulic performance of alternate twisted tape are superior to typical twisted tapes under similar operating conditions.

Naik et al. [37] examined the convective heat exchange improvement and friction factor behaviors in channel inserted with twisted tape and using CuO-water nanofluids with different

concentrations of 0.25%, 0.1% and 0.5% by volume as the working fluids. The use of twisted tape with the nanofluid with concentrations of 0.5% by volume resulted in the maximum increases of heat exchange rate by 76% and friction penalty by 26.6% as evaluated to those of the base fluid. Morteza and Eskandari [38] combined the consequences of non-uniform twisted tape and Cu-water nanofluid for heat exchange augmentation. Their result indicated that the twisted tape together with Cu-water nanofluid (0.3. wt. %) enriched the overall improvement ratio up to 87%. Maddah et al. [39] executed assessments to study the heat exchange augmentation by customized twisted tapes with different geometrical progression ratios (GPR) and Al2O3-water nanofluid. Their results showed that the use of the reducer geometrical progression ratio (RGPR<1) with Al2O3-water nanofluid could promote heat transfer up to 52% as compared to those of the typical twisted tape.

Bhattacharyya et al. [40,41] and Saha et al. [42] experimentally studied center-cleared twisted tapes with artificial rib roughness and achieved considerably higher than the individual enrichment method individually for laminar regime flow through a circular channel up to a definite quantity of twisted-tape center-clearance. Bhattacharyya et al. [43,44] reported on numerical work circular twisted tape elliptical twisted tube type swirl producers. Thianpong et al. [45] assessed compound heat exchange improvement methods of a dimpled tube with twisted tape inclusions. Mengna et al. [46] reported on thermo-hydraulic consequences of a converging-diverging channel with tape inserts. Sivashanmugam et al. [47] experimentally reported on thermo-hydraulic characteristics of laminar flow in circular channel fitted with screw tape.

The foremost intention of the present work is to experimentally determine the thermo-hydraulic performance of corrugated tubes with spring tape inserts as a measure to further enhance the heat transfer in turbulent forced convection. Air is used as the working fluid. The investigation is performed for a Reynolds number range between 10,000 and 50,000.

In the reviewed literature, one can see that corrugated tubes lead to an increase of the Nusselt number compared to the plain tube, however, with an over-proportional increase of the pressure drop, leading to thermo-hydraulic performance values smaller than unity. In the present work, we combine the corrugated tube with a spring tape, in effort of obtaining a configuration with improved thermo-hydraulic performance. The work is innovative in so far, that this combination, i.e. corrugated tubes with spring tape, has not been investigated by the researchers before. On the other hand, there has been considerable work on twisted tapes, ribs, delta winglet inserts, and etc. in various types of modified tubes [48]. The special feature of the present configuration, which relies on a spring tape, compared to the mentioned alternative arrangements, lies in its simplicity in production and application.

2. The experimental rig and the procedure

Fig. 1 shows the schematic diagram of the experimental setup. The atmospheric air is sucked by a 7.0 kW blower. After passing through a poly vinyl chloride made pipe and an adjustable bypass valve, the air flow reaches a rotameter that can measure flow rates varying between 120 and 540 liters per hour, with an error of 0.052%. The air velocity was continuously adjusted by adjusting the valve opening to obtain approximately the same Reynolds numbers for the different cases. A U-tube manometer is used to measure the pressure drop across the test section. In order to measure the pressure drop, two pressure taps are placed at inlet and outlet of the test section, with a net distance of 2.10 m in between, and differential U-tube manometer is used, ranging from 0 -150 mm Hg. Steady-state conditions were reached one and half hours after start-up. Steady-state conditions were assumed once there was no significant change in the mass flow rate, temperature, current, pressure drop and the energy balance readings.

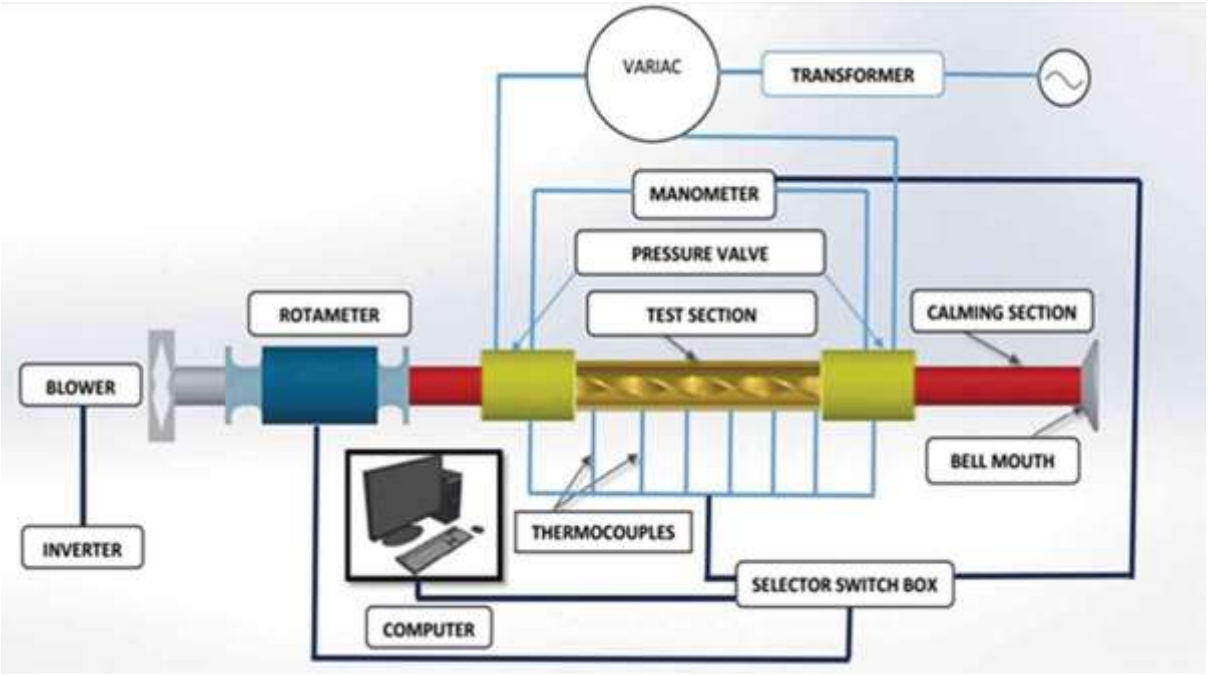

Fig.1. Schematic diagram of experimental setup

The heat transfer test section was electrically heated by a nichrome heater wire wrapped around the tube wall, covered by a porcelain bead insulation preventing a direct contact with the duct wall. Fiber glass, glasswool, asbestos layers are applied to the test section that are finally covered by a jut bag. A selector switch box is used to measure the temperature of the inlet and outlet test section and the duct wall temperatures. The wall temperature is measured by 28 copper-constantan thermocouples that are fitted on the tube outside wall by brazing. The thermocouples are installed at 7 axial locations distributed equidistantly along the tube length. At each axial position, 4 thermocouples are used that are equidistantly placed around the circumference. The high thermal conductivity of the tube wall out of brass (124 W/mK) facilitated to achieve a quite uniform inner wall temperature with variations remaining below ±4%. Specifications of some major measuring instruments are shown in Table 1 and uncertainties of some major experimental variables are given in Table 2. The uncertainty in Reynolds number, friction factor and Nusselt number were estimated as ± 4.1 %, ± 5.4 % and ± 6.4 %, respectively following the procedure of Saha et al. [42].

Table 1. Specifications of major measuring instruments.

Instruments	Range
DC power supply	0–1,500 W
Thermocouples	−100°C to 350°C
Rotameter	i) 0–120 L/h, and ii) 0–540 L/h
U-tube Manometer	0–150 mm Hg

Table 2. Uncertainties of major parameters.

Name of variables	Errors (%)
Flow velocity, v	0.18
Voltage on the heater, V	0.15
Electrical resistance, R	0.33
Heat transfer coefficient, h	1.19
Current on the heater, I	0.23
Ambient temperature, T_a	0.1
Electrical power on the heater, P	0.17
Average temperature, T	0.6

For validation purposes, the experiment is carried out, first, in a circular plane tube without any corrugation and inserts. This baseline tube geometry has an inner diameter (D) of 22.0 mm and a length (L) of 2.0 m. The geometry of the corrugated tube is displayed in Fig. 2. In choosing the size and arrangement of the tube and tape inserts is, we have been inspired by the work of Thianpong et al. [45], who investigated twisted tape inserts. In difference to this work, we are investigating, however, the applicability of a tape in the form of a spring, which has never been examined before, although it is essentially the simplest configuration of a tape insert.

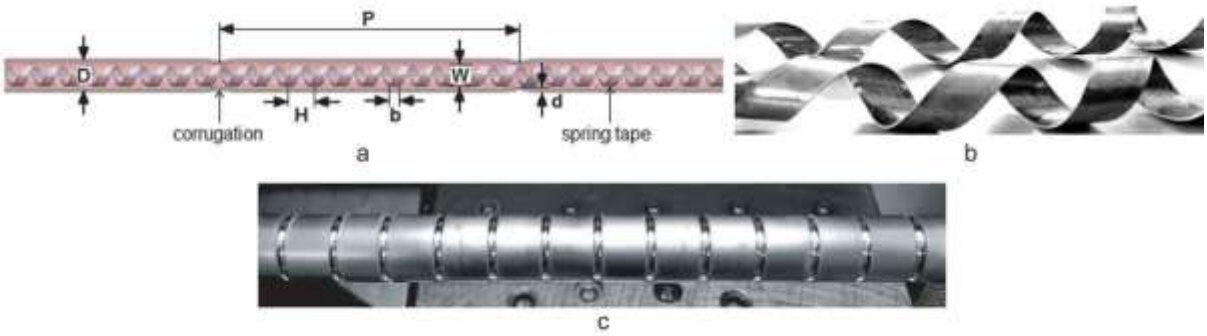

Fig. 2. Views of corrugated tube with spring tape insert, (a) layout of a corrugated tube in combination with spring tape insert, (b) photographic view of spring tape, (c) photographic view of corrugated tube

The corrugation depth (d) is kept at 3.0 mm, while different numbers of corrugations are used along the tube length, with a pitch (P). The corrugation "pitch ratio" (y) is defined as y=P/D. Two values of the pitch ratio are investigated: y = 0.7, 1.0. The spring material has a flat cross section (5.7 mm x 1.0 mm) and is winded to lead to a spring diameter of 12 mm, which is called, here as the width (W) of the spring. The pitch between the windings is denoted by H, and a "spring ratio" (s) is defined as s=H/W. Three values of the spring ratio are investigated: s = 3.0, 5.0, 7.0.

3. Data reduction

The rate of heat transferred to the air, Q , is obtained from

$$Q = m\, c_p\, (T_o - T_i) \tag{1}$$

where m and $C_{p,}$ denote the mass flow rate and the mean isobaric specific heat capacity of air, while T_i and T_o stay for the inlet and outlet temperatures, respectively.

The energy balance error (EBE*)*, was used to compare the measured heat transfer with the electrical energy supplied, Q_e=IV, and is given as :

$$\mathrm{EBE} = \left[\frac{Q_e - Q}{Q_e}\right] \times 100 \tag{2}$$

The average EBE for the entire experimental investigation was less than 2.5% -3.0%, which was considered to be due to the heat leakage from the duct wall

The wall heat flux, q_w, is calculated by

$$q_w = \frac{Q}{A} \tag{3}$$

where, A is the tube inner wall surface area.

The bulk fluid temperature, T_b, is calculated as the arithmetic average of the inlet outlet temperatures as

$$T_b = \frac{T_o + T_i}{2} \tag{4}$$

The average temperature at the outer tube wall, T_{ow}, is obtained from the arithmetic average of all temperatures measured by the thermocouples. The average inner wall temperature, T_w, is, then, obtained from the average outer wall temperature (T_{ow}) using the measured heat flow rate (Q) and the tube wall thermal resistance (R_w) from

$$T_w = T_{ow} - QR_w \tag{5}$$

The tube wall thermal resistance is calculated form the outer and inner tube diameters (D_o, D), tube length (L) and the thermal conductivity of the tube material (brass) tube as:

$$R_w = \frac{\ln(D_o/D)}{2\pi k_{BRASS} L} \tag{6}$$

The heat transfer coefficient, h [1], is, then calculated as,

$$h = \frac{q_w}{T_w - T_b} \tag{7}$$

and the Nusselt number (Nu) [1] is obtained from

$$Nu = \frac{h\,D}{k} \tag{8}$$

where k denotes the fluid thermal conductivity.

The Darcy friction factor (f) [1] is evaluated from

$$f = \frac{\Delta p}{\frac{L}{D}\frac{1}{2}\rho V^2} \tag{9}$$

In the above equation, Δp and ρ denote the static pressure drop across the tube and fluid density, respectively, while V denotes the bulk fluid velocity based on the turbulator-free and uncorrugated tube cross-section. The Reynolds number (Re) is also defined based on the inner diameter (D) of the turbulators-free and uncorrugated plain tube and V. The air material properties are evaluated at the bulk fluid temperature (T_b).

For a combined assessment of the heat transfer augmentation and the associated pressure drop, the thermo-hydraulic performance factor (η) suggested by Chang et al. [24] is used:

$$\eta = \frac{Nu / Nu_0}{(f / f_0)^{0.33}} \tag{10}$$

where the subscript 0 denotes the turbulator and corrugation free, circular plain tube.

4. Results and discussion

As an initial step, a smooth tube without any turbulator is investigated experimentally. As the present configuration (with L/D = approx. 45) does not necessarily imply a fully develop flow throughout, the present measurements are compared with the correlations proposed by by Thianpong et al. [45] for developing pipe flow based on the measurements obtained on a similar configuration. The comparisons of the measured Nusselt numbers (Nu), and friction factors (f) with the correlations of Thianpong et al. [45] are presented in Fig. 3. A very close agreement between the present measurements and correlations can be observed (Fig. 3).

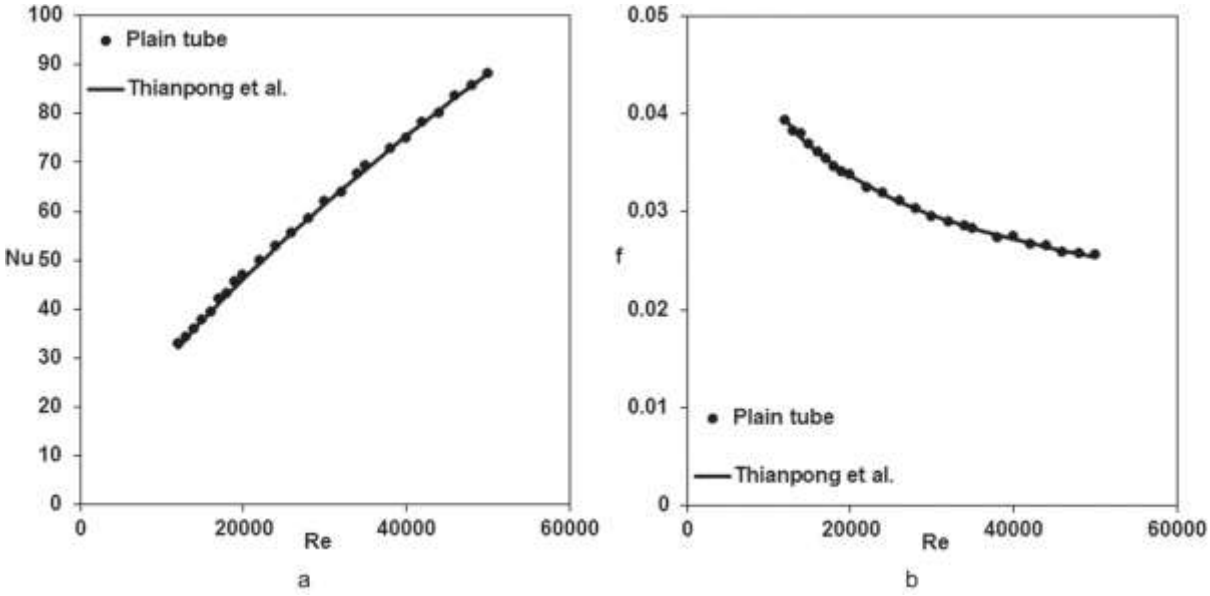

Fig. 3 Measurements compared with correlations of Thianpong et al. [45] for plain tube without insterts (a) Nusselt number, (b) friction factor

The effect of the corrugation pitch ratio (y=0.7 and 1.0) on the Nusselt number without and with spring tape (for s=3.0) is shown in Fig. 4(a). As expected, all cases exhibit an increase in Nusselt number with increasing Reynolds number, and all geometry augmentations provide an increase of Nusselt number compared to the plain tube without inserts. While the heat transfer enhancement for y=1.0 without spring tape is only marginal compared to the plain tube, a reduction of the corrugation pitch ratio to y=0.7 achieves a remarkable increase in Nu as this geometry (y=0.7) is more effective in interrupting the boundary layer and increasing turbulence intensity compared to the case with y =1.0. Insertion of the spring tape with s=3.0 causes an additional, and substantial increase in the Nusselt number, due to the additional turbulation by the spring tape and the induced secondary, swirling flows. The dependence of the Nusselt number on the corrugation pitch ratio y, is observed to be similar without and with spring tape (s=3.0). Fig. 4(b) presents the results for the friction factor, corresponding to the cases considered in Fig. 4(a). As expected, the friction factors decrease with increasing Re, and the cases with higher Nu are more strongly penalized in terms of the friction factor. The

assessment of the overall performance will be presented, later on, based on the thermo-hydraulic performance parameter.

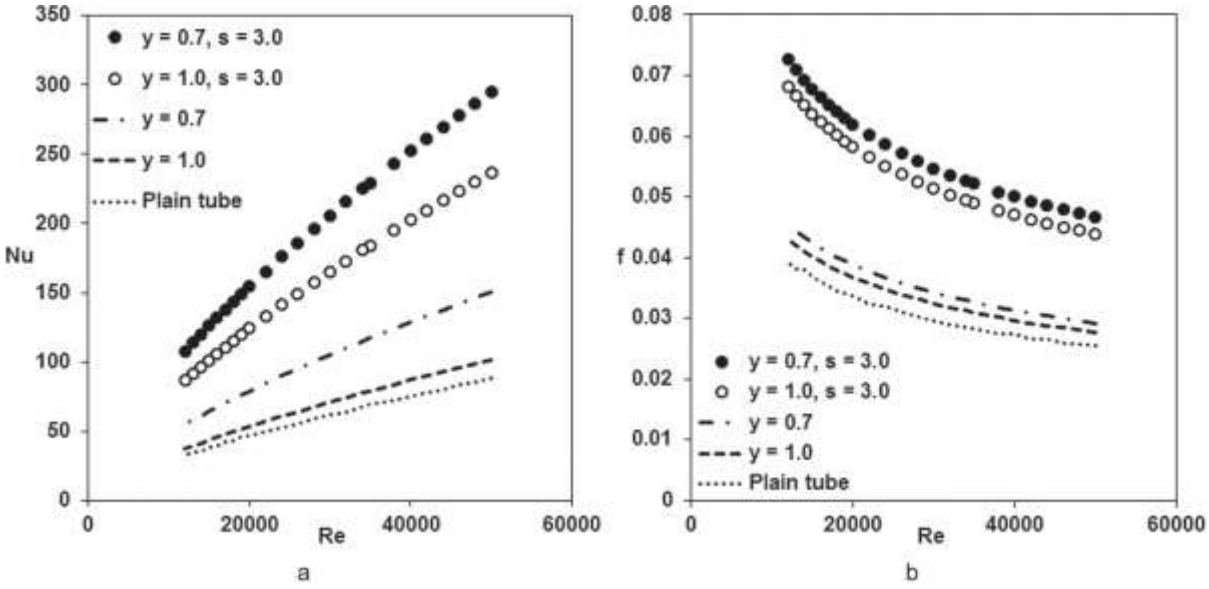

Fig. 4 Effect of pitch ratio (a) Nusselt number, (b) friction factor.

Fig. 5 shows the effect of the spring ratio (s =3.0, 5.0 and 7.0) for corrugated tubes with the pitch ratios y=1.0 (Fig. 5(a)) and y=0.7 (Fig. 5(b)). The Nusselt number (Fig. 5a) increases as the Reynolds number increases, and this trend gets stronger with decreasing spring ratio. For the same Reynolds number, the Nusselt number increases with the decreasing spring ratio. This is due to increasing turbulence intensity, swirl generation and, also, residence time with the decreasing spring ratio. For the higher pitch ratio (y=1.0), a considerably large heat transfer enhancement is already achieved by the insertion of the spring tape with largest spring ratio (s=7.0), where a further decrease of the spring ratio is observed to cause rather marginal increases of the Nusselt number (Fig. 5(a)). In comparison, for the lower pitch ratio (y=0.7), the case with the largest spring ratio (s=7.0) does not seem to cause a that abrupt increase of the Nusselt number, but seems to approximately double the effect of the corrugated case without inserts. Further decreases of the spring ratio affects the Nusselt number also more remarkably (Fig. 5(b)), in comparison.

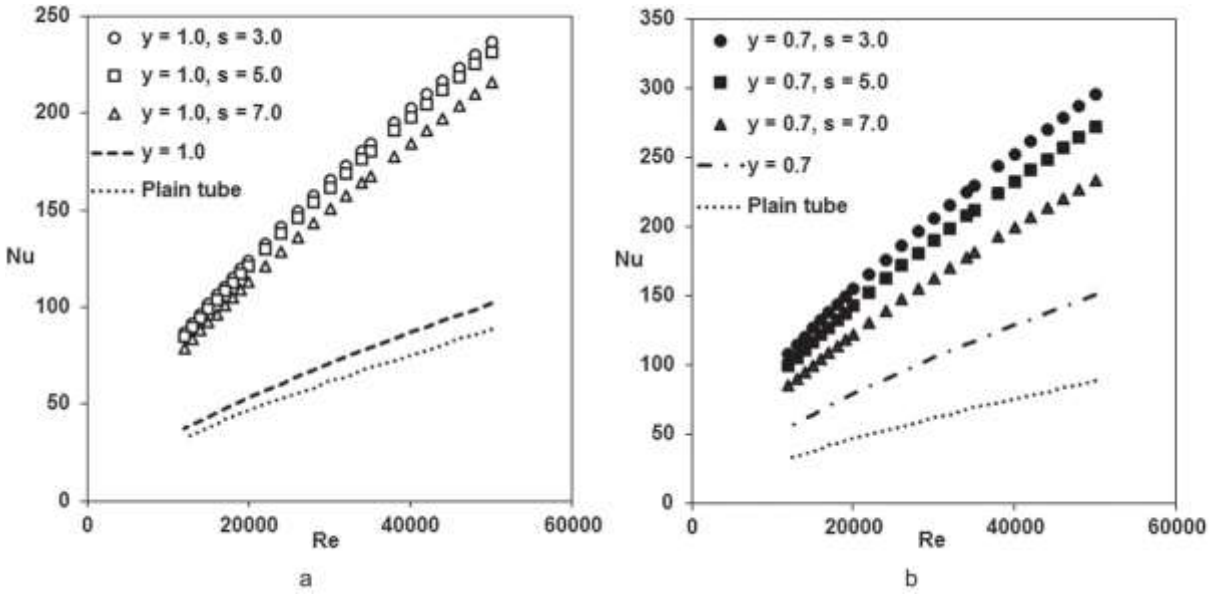

Fig. 5 Effect of spring ratio (a) Nusselt for y=1.0, (b) Nu for y = 0.7

The results of all investigated cases are presented, collectively, in Fig. 6. Corrugation of the tube without spring tape leads to a comparably moderate heat transfer enhancement, whereas the insertion of spring inserts allows larger values to be achieved. One can see that the combination of the low spring and low pitch ratios lead to larger Nusselt numbers, and friction factors (which was also obvious in the previous comparisons). Please note that the cases with high pitch ratio and low spring ratio (y=1.0, s=3.0) and low pitch ratio and high spring ratio (y=0.7, s=7.0) lead to very similar Nusselt numbers, so that the curves are practically covering each other (Fig. 6a). For the friction factor, this situation (very close values) is observed between the cases y=0.7, s=5.0 and y=0.7, s=5.0. For pure tube wall corrugation without inserts, an increase of the Nusselt number of about 15% is obtained for y=1.0 where this ratio becomes approx. 70% for y=0.7, compared to the plain tube. With spring tape inserts, the weakest Nusselt number increase is given by the case y=1.0, s=7.0, which offers an enhancement of about 145% compared to the plain tube. The strongest increase of the Nusselt number is provided by the case y=0.7, s=3.0 which leads to an increase of the Nusselt number of approx. 235%, overall, compared to the plain tube.

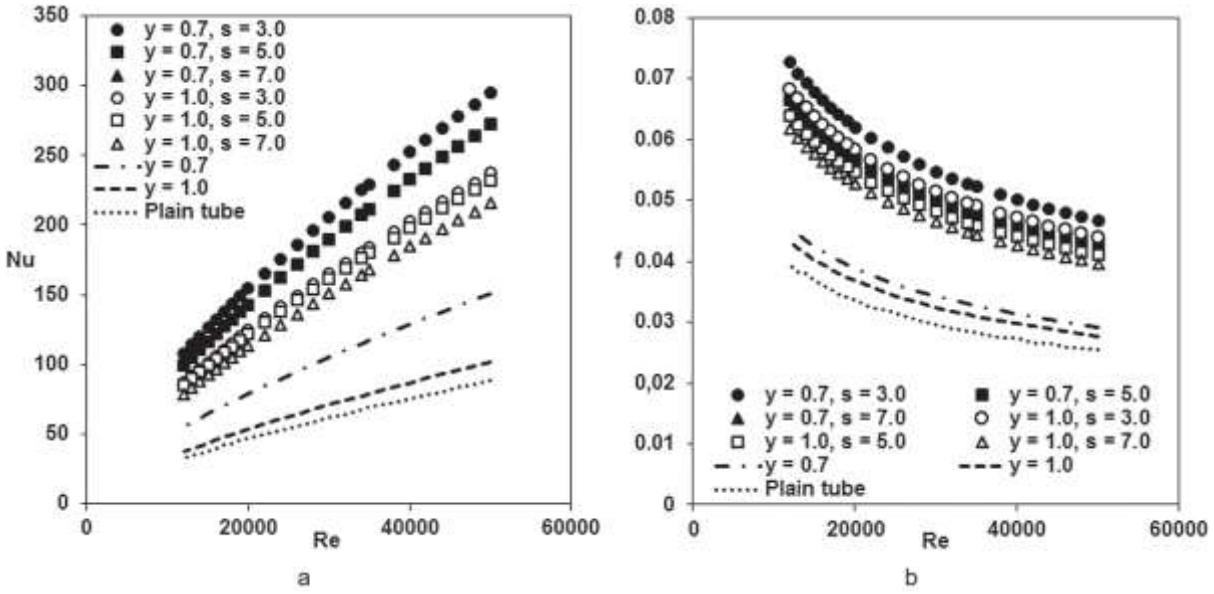

Fig. 6 Collective representation of results (a) Nusselt number, (b) friction factor

The Nusselt numbers and friction factors of the investigated cases in comparison to those of the plain tube are presented in Fig: 7, in terms of the ratios Nu/Nu_0 (Fig. 7a) and f/f_0 (Fig. 7b). One can see that both parameters don't necessarily show a significant Reynolds number dependence, apart from local fluctuations. It can be seen in Fig. 7a that the use of small values of pitch and spring ratio leads to an increase in Nu/Nu_0, while the rise of pitch and spring ratio yields the reduction of the Nu/Nu_0 values. In Fig. 7b, one can visualize that the rise in the pitch and spring ratio value results in lower f/f_0 values, whereas small pitch and spring ratios lead to higher f/f_0.

An overall assessment of the heat transfer enhancement can be achieved by the thermo-hydraulic performance factor, η, (Eq. 10). The variations of thermal performance factor with Reynolds number for corrugated tubes with spring tape inserts are presented in Fig. 7. It is interesting to note that the thermo-hydraulic performance seems to be nearly independent of the Reynolds number for all cases considered, and all geometry augmentations lead to a performance improvement, i.e. to $\eta > 1$.

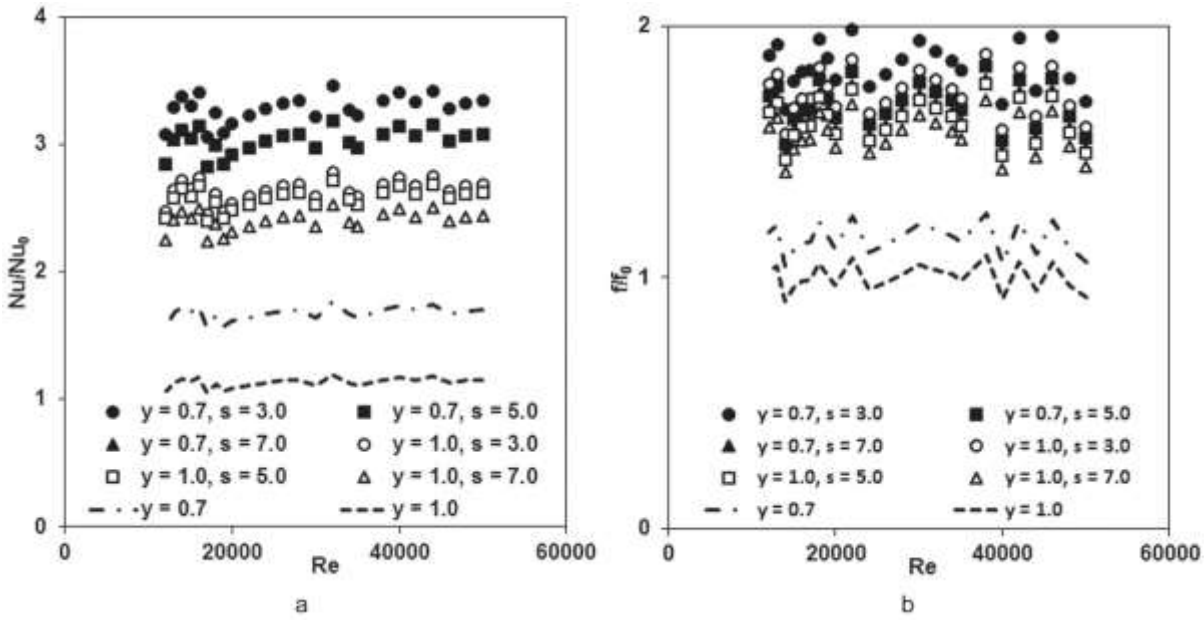

Fig. 7 Ratios of Nusselt numbers and friction factors (a) Nu/Nu_0, (b) f/f_0

The performances of the three cases: y=1.0, s=5.0; y=1.0, s=3.0; y=0.7, s=7.0 turn out to be very similar so that their curves in Fig. 8 are nearly congruent. The highest performance parameter, approx. 2.8, is observed for the case y=0.7, s=3.0. The performance of the case with y=0.7, s=5.0 is smaller, but rather close. Roughly, one can recognize four performance categories, with rather small internal differences compared to the others: 1) plain tube and y=1.0 (without spring tape); 2) y=0.7 (without spring tape); 3) y=1.0, s=7.0; y=1.0, s=5.0; y=1.0, s=3.0 and y=0.3, s=7.0; 4) y=0.7, s=5.0 and y=0.7, s=3.0. The performance improvement from one category to the next turns out to be similar, i.e. by increments of approx. 0.6.

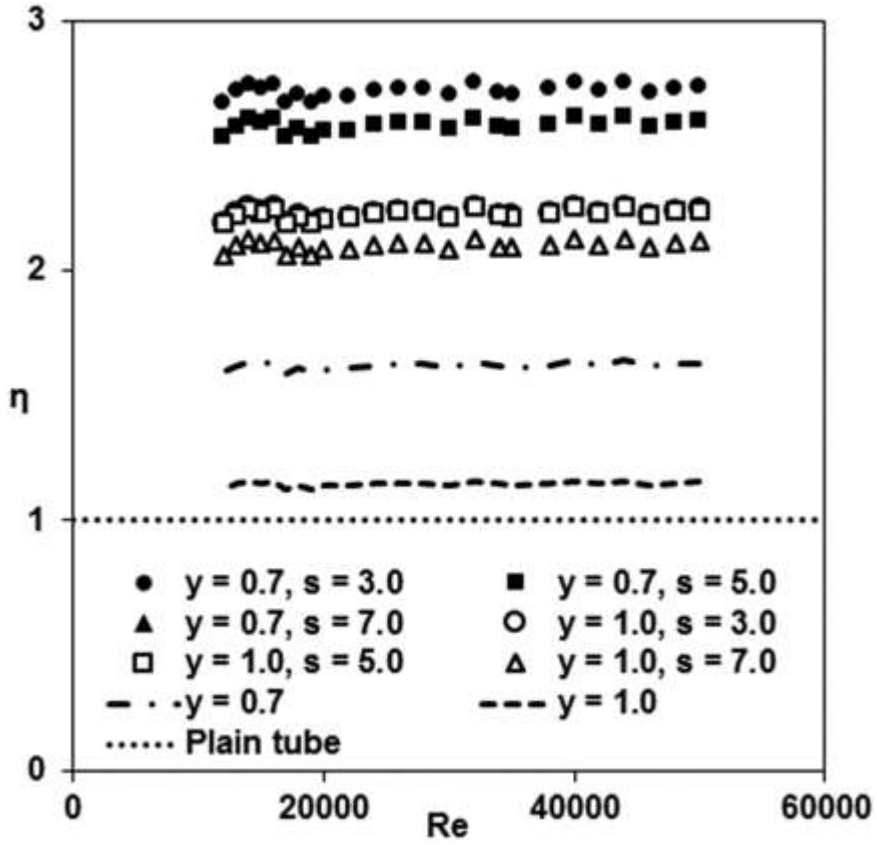

Fig. 8 Thermo-hydraulic performance parameter

The experimental results can be used to derive correlations for corrugated tubes with spring tape inserts, which express the Nusselt number (Nu) and the friction factor (f) that as functions of the Reynolds number (Re), the pitch ratio (y) and the spring ratio (s). These correlations that are derived for turbulent forced convection through corrugates tubes with spring tape inserts, for the presently considered range of parameters ($10^4 \leq \mathrm{Re} \leq 50^4$; $\mathrm{Pr} \approx 0.7$; $0.7 \leq y \leq 1.0$; $3.0 \leq s \leq 7.0$) are provided below.

$$\mathrm{Nu} = 0.15\,\mathrm{Re}^{0.71}\,y^{-0.11}\,s^{-0.21} \tag{11}$$

$$f = 1.42\,\mathrm{Re}^{-0.31}\,y^{-0.14}\,s^{-0.13} \tag{12}$$

Please note that the Nusselt number depends, in general, on the Prandtl number too [1]. However, the present experiments have been carried out for the same fluid, i.e. for air, where the differences in the bulk fluid temperatures have also not been leading to any significant variations in the Prandtl number to provide a basis for a correlation. Therefore, the Nusselt number correlation given by Eq. (11) does not embody a Prandtl number dependence, and is valid for Pr ≈ 0,7 (e.g. atmospheric air for bulk fluid temperatures between approx. 300 K – 700 K).

The above correlations for the Nusselt number (5) and the friction factor (6) are compared with the experimental values in Fig. 9. One can see that the correlations agree quite well with the experimental data, within approx. ±10% deviation for the Nusselt number and ±5% for the friction factor.

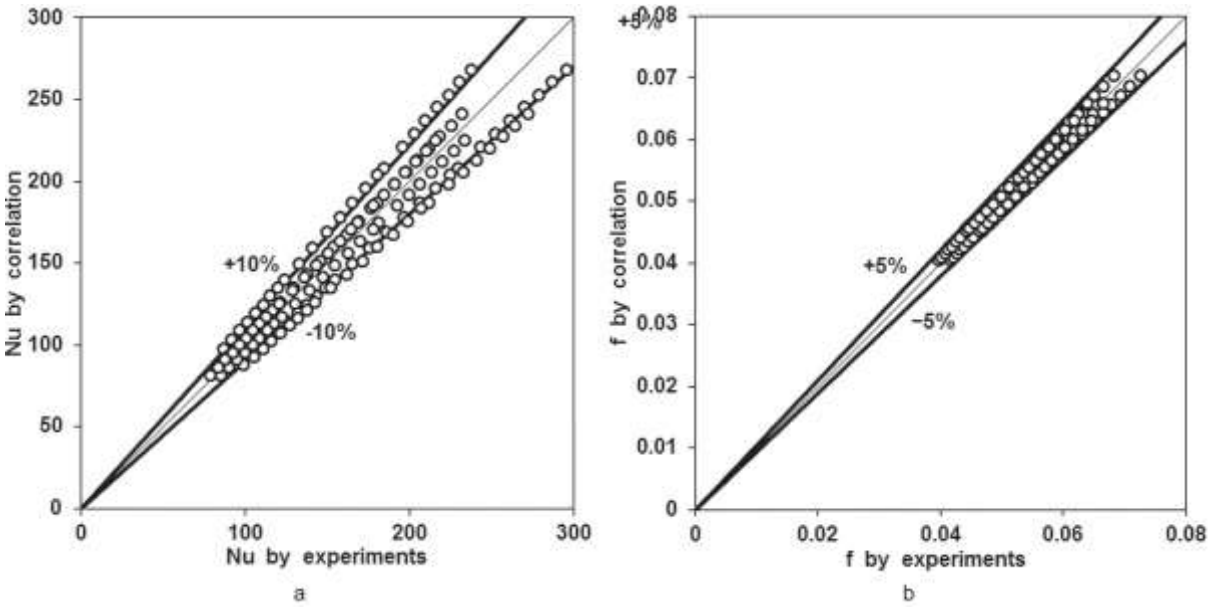

Fig. 9 Comparison of proposed correlations with experimental data (a) Nusselt number, (b) friction factor

In Figure 10, the thermo-hydraulic performance obtained provided by the present configuration is compared with the thermo-hydraulic performances of different configurations out of the literature. For comparison, the following configurations are selected: corrugated tube [49], finned tube [50], twisted tri-lobed tube [51], propeller type swirl generator [52], double

helical tape [53], wire coil inserts [54], broken twisted tape [55], multiple square perforated twisted tape (TT) [56], and V-pattern dimple obstacle [57]. Usually, a range of thermo-hydraulic performance factors is always obtained, depending on the parameter variations of the considered configuration, like in present study (Fig. 8). Thus, a direct comparison of different configurations is not very straightforward. In the present comparison (Fig. 10), the maximum values obtained for each configuration are considered. One can see that the present configuration performs quite well, providing higher thermo-hydraulic performance values compared to many of the alternative configurations. The double helical tube of Bhuiya et al. [53] performs similar to the present configuration for the lower values of the Reynolds number of its considered range (Re ~ 30000) and performs increasingly better for increasing Re. However, its performance for lower Reynolds numbers (Re < 30000) is not evidenced, whereas the present data covers also lower Reynolds numbers. Multiple square perforated twisted tape of Suri et al. [56] and V-pattern dimple objects of Kumar et al. [57] show a better performance compared to the present configuration. These configurations are, however, tested for rather low Reynolds numbers (Re < 20000 for [56], Re < 30000 for [57]), whereas the present data covers a broader range of Reynolds numbers including larger values up to 50000. It shall also be emphasized again that the present configuration relying on a spring tape is much simpler to design, produce and install compared to the devices encountered in alternative arrangements [53, 56, 57]. Thus, the present configuration can be considered to be a useful alternative for heat transfer enhancement.

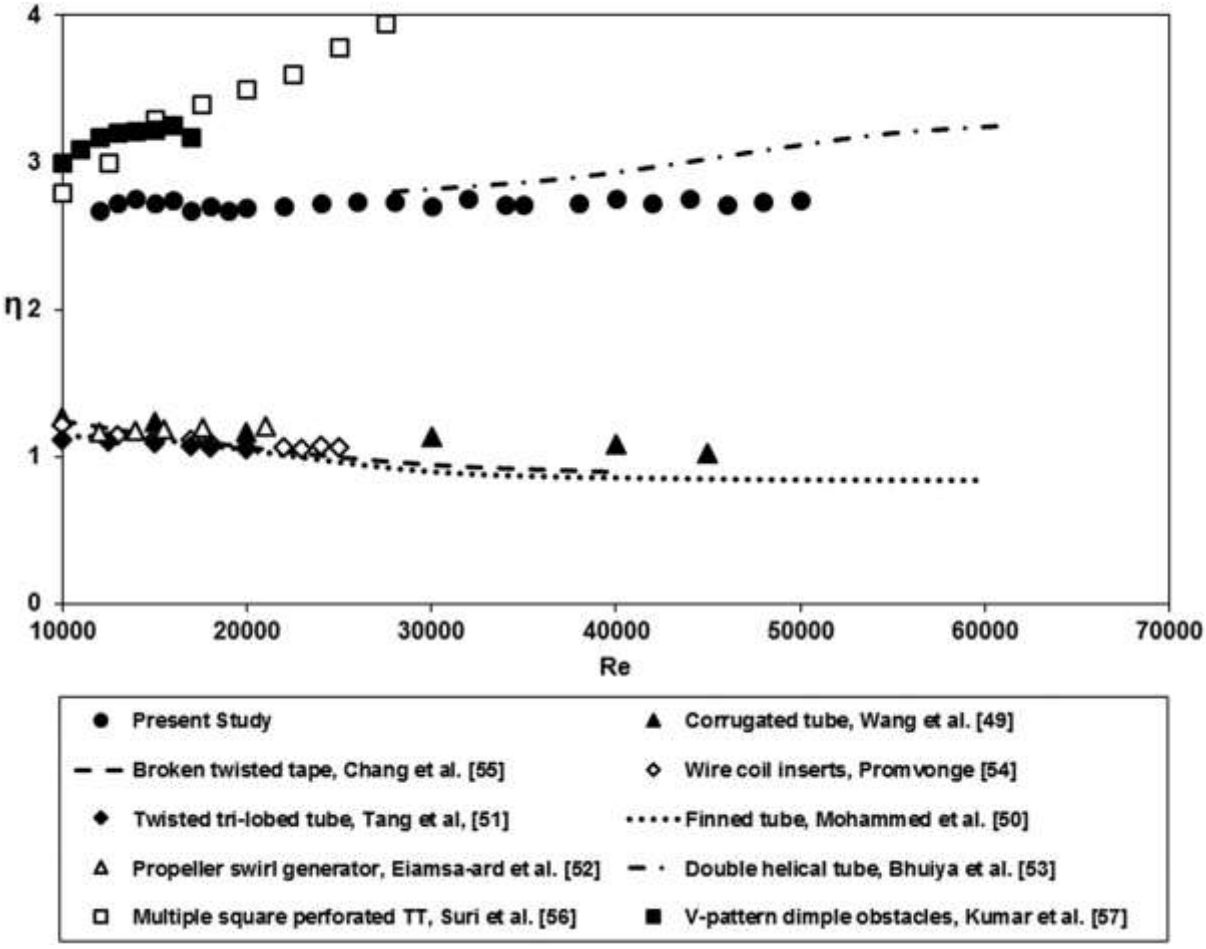

Fig. 10 Comparison of presently obtained thermo-hydraulic performance values with previous studies

5. Conclusions

Experimental investigations of turbulent flow and heat transfer in a corrugated tube in combination with spring tape inserts are performed. The impacts of the pitch ratio, y, and the spring ratio, s, on thermo-hydraulic characteristics are analyzed. The Nusselt number and the friction fsctor are observed to increase with y and s. It is observed that the thermo-hydraulic performance parameter, η, increases for all considered geometry modifications, within the lowest value of approx. η=1.2 for the corrugated tube without spring tape insert with y=1.0, and the highest value of approx. η=2.8 for the corrugated tube with spring tape insert with y=0.7, s=0.3. Predictive correlations for the Nusselt number and the friction factor for the investigated cases are proposed.

Acknowledgement

The authors would like to gratefully acknowledge Sam Casting, MCKV Institute of Engineering (MCVIE) and Jadavpur University, India for their support in this research.

References

1. R.K. Shah and D.P. Sekulic, *Fundamentals of Heat Exchanger Design*, Hoboken, New Jersey, USA: John-Wiley & Sons, 2007.

2. A. Yutaka, N. Hiroshi and M. Faghri, "Heat transfer and pressure drop characteristics in a corrugated duct with rounded corners", *Int. J. Heat Mass Transf.*, vol. 31, no. 6, pp. 1237-1245, June 1988. doi: 10.1016/0017-9310(88)90066-X.

3. A.C. Benim, M. Cagan and D. Günes, "Computational analysis of transient heat transfer in turbulent pipe flow", *International Journal of Thermal Sciences*, vol. 43, no. 8, pp. 725-732, August 2004. doi:10.1016/j.ijthermalsci.2004.02.012.

4. A.C. Benim, D. Brillert and M. Cagan, "Investigation into the computational analysis of direct-transfer pre-swirl systems for gas turbine cooling", ASME Paper No. GT2004-54151 Proc. ASME Turbo Expo 2004, Vienna, Austria, June 14-17, 2004, vol. 4, pp. 453-460, 2004. doi:10.1115/GT2004-54151.

5. A.C. Benim, K. Ozkan, M. Cagan and D. Gunes, "Computational investigation of turbulent impinging jet onto rotating disk", *International Journal of Numerical Methods for Heat and Fluid Flow*, vol. 17, no. 3, pp. 284-301, 2007. doi:10.1108/09615530710730157.

6. H. Chattopadhyay and A.C. Benim, Turbulent heat transfer over a moving surface due to impinging slot jets, *Journal of Heat Transfer – Transactions of the ASME* , vol. 133, no. 10, Article Number: 104502, 5 pages, 2011. doi:10.1115/1.4004075.

7. A.C. Benim, H. Chattopadhyay and A. Nahavandi, "Computational analysis of turbulent forced convection in a channel with a triangular prism", *International Journal of*

Thermal Sciences, vol. 50, no. 10, pp. 1973-1983, October 2011. https://doi.org/10.1016/j.ijthermalsci.2011.05.002.

8. J.P. Meyer and J.A. Olivier, "Transitional flow inside enhanced tubes for fully developed and developing flow with different types of inlet disturbances: Part I - Adiabatic pressure drops", *Int. J. Heat Mass Transf.*, vol. 54, no. 7-8, pp. 1587– 1597, March 2011. doi:j.ijheatmasstransfer.2010.11.027.

9. J.P. Meyer and J.A. Olivier, "Transitional flow inside enhanced tubes for fully developed and developing flow with different types of inlet disturbances: Part II-heat transfer", *Int. J. Heat Mass Transf.*, vol. 54, no. 7-8, pp. 1598–1607, March 2011. doi:10.1016/j.ijheatmasstransfer.2010.11.026.

10. S. Bhattacharyya, H. Chattopadhyay and A.C. Benim, "Heat transfer enhancement of laminar flow of ethylene glycol through a square channel fitted with angular cut wavy strip", *Procedia Engineering*, vol. 157, pp.19-28, 2016. doi:10.1016/j.proeng.2016.08.333.

11. S. Bhattacharyya, H. Chattopadhyay and A.C. Benim, "Computational investigation of heat transfer enhancement by alternating inclined ribs in tubular heat exchanger", *Progress in Computational Fluid Dynamics*, vol. 17, no. 6, pp. 390-396, 2017. https://doi.org/10.1504/PCFD.2017.088818.

12. J.P. Meyer and S.M. Abolarin, "Heat transfer and pressure drop in the transitional flow regime for a smooth circular tube with twisted tape inserts and a square-edged inlet", *Int. J. Heat Mass Transf.*, vol. 117, pp. 11–29, February 2018. doi:j.ijheatmasstransfer.2017.09.103.

13. A.C. Benim, A. Nahavandi and K.J. Syed, "URANS and LES analysis of turbulent swirling flows", *Progress in Computational Fluid Dynamics*, vol. 5, no. 8, pp. 444-454, 2005. https://doi.org/10.1504/PCFD.2005.007680.

14. B.A. Sarac and T. Bali, "An experimental study on heat transfer and pressure drop characteristics of decaying swirl flow through a circular pipe with a vortex generator", *Exp.*

Therm. Fluid Sci., vol. 32, no. 1, pp. 158–165, October 2007. doi:10.1016/doi:j.expthermflusci.2007.03.002.

15. S. Eiamsa-ard and P. Promvonge, "Influence of double-sided delta-wing tape insert with alternate-axes on flow and heat transfer characteristics in a heat exchanger tube", *Chinese J. Chem. Eng.*, vol. 19, no. 3, pp. 410–423, June 2011. doi:10.1016/S1004-9541(11)60001-3.

16. P.W. Deshmukh and R.P. Vedula, "Heat transfer and friction factor characteristics of turbulent flow through a circular tube fitted with vortex generator inserts", *Int. J. Heat Mass Transf.*, vol. 79, pp. 551–560, December 2014. doi:10.1016/j.ijheatmasstransfer.2014.08.042.

17. K. Song, Z. Xi, M. Su, L. Wang, X. Wu and L. Wang, "Effect of geometric size of curved delta winglet vortex generators and tube pitch on heat transfer characteristics of fin-tube heat exchanger", *Exp. Therm. Fluid Sci.*, vol. 82, pp. 8–18, April 2017. doi:10.1016/j.expthermflusci.2016.11.002.

18. Y. Xu, M.D. Islam and N. Kharoua, "Numerical study of winglets vortex generator effects on thermal performance in a circular pipe", *Int. J. Therm. Sci.*, vol. 112, pp. 304–317, February 2017. doi:10.1016/j.ijthermalsci.2016.10.015.

19. M. Fiebig, A. Valencia and N.K. Mitra, "Local heat transfer and flow losses in fin-tube heat exchangers with vortex generators: a comparison of round and flat tubes", vol. 8, no. 1, pp. 35-45, January 1994. doi:10.1016/0894-1777(94)90071-X.

20. S. Roy and S.K. Saha, "Thermal and friction characteristics of laminar flow through a circular duct having helical screw-tape with oblique teeth inserts and wire coil inserts", *Exp. Therm. Fluid Sci.*, vol. 68, pp. 733–743, November 2015. doi:10.1016/j.expthermflusci.2015.07.007.

21. L.S. Sundar, P. Bhramara, N.T.R. Kumar, M.K. Singh and A.C.M. Sousa, "Experimental heat transfer, friction factor and effectiveness analysis of Fe3O4 nanofluid flow in a horizontal plain tube with return bend and wire coil inserts", *Internat. J. Heat Mass Transf.*,

vol. 109, pp. 440–453, June 2017, doi:10.1016/j.ijheatmasstransfer.2017.02.022.

22. O. Keklikcioglu and V. Ozceyhan, "Experimental investigation on heat transfer enhancement of a tube with coiled-wire inserts installed with a separation from the tube wall", *Int. Comm. Heat Mass Transf.*, vol. 78, pp. 88–94, November 2016. doi:10.1016/j.icheatmasstransfer.2016.08.024.

23. S.K. Saha and D.N. Mallick, "Heat transfer and pressure drop characteristics of laminar flow in rectangular and square plain ducts and ducts with twisted-tape inserts", *J. Heat Transf.*, vol. 127, no. 9, pp. 966–977, November 2004. doi:10.1115/1.2010493.

24. S.W. Chang, L.M. Su, T.L. Yang and S.F. Chiou, "Enhanced heat transfer of shaker bored piston cooling channel with twisted tape insert", *Heat Transf. Eng*., vol. 28, no. 4, pp. 321–334, 2007. doi:10.1080/01457630601122740.

25. H.A. Mohammed, H.A. Hasan and M.A. Wahid, "Heat transfer enhancement of nanofluids in a double pipe heat exchanger with louvered strip inserts", *Int. Comm.. Heat Mass Transf.*, vol. 40, pp. 36–46, January 2013. doi:10.1016/j.icheatmasstransfer.2012.10.023.

26. I. Yaningsih, T. Istanto and A.T. Wijayanta, "Experimental study of heat transfer enhancement in a concentric double pipe heat exchanger with different axial pitch ratio of perforated twisted tape inserts", *AIP Conf. Proc.*1717, 030012, 2016. doi: 10.1063/1.4943436.

27. I. Yaningsih and A.T. Wijayanta, "Influences of pitch-length louvered strip insert on thermal characteristic in concentric pipe heat exchanger", *MATEC Web of Conferences,* vol. 101, Article Nr.: 03014, 5 pages, March 2017. doi:10.1051/matecconf/201710103014.

28. N.M. Zade, S. Akar, S. Rashidi and J.A. Esfahani, "Thermo-hydraulic analysis for a novel eccentric helical screw tape insert in a three-dimensional tube", *Appl. Therm. Eng.*, vol. 124, pp. 413–421, September 2017. doi:10.1016/j.applthermaleng.2017.06.036.

29. I. Yaningsih, A.T. Wijayanta, "Concentric tube heat exchanger installed by twisted tape using various wings with alternate axis",*AIP Conf.Proc.*1788,030005,2017.doi: 10.1063/1.4968258

30. K. Wongcharee and S. Eiamsa-ard, “Enhancement of heat transfer using CuO/water nanofluid and twisted tape with alternate axis”, *Int. Comm. Heat Mass Transf.*, vol. 38, no. 6, pp. 742-748, July 2011. doi:10.1016/j.icheatmasstransfer.2011.03.011.

31. S. Eiamsa-ard, C. Thianpong and P. Promvonge, “Experimental investigation of heat transfer and flow friction in a circular tube fitted with regularly spaced twisted tape elements”, *Int. Comm. Heat Mass Transf.*, vol. 33, no. 10, pp. 1225-1233, December 2006. doi:10.1016/j.icheatmasstransfer.2006.08.002.

32. S. Eiamsa-ard, C. Thianpong, P. Eiamsa-ard and P. Promvonge, “Convective heat transfer in a circular tube with short-length twisted tape insert”, *Int. Comm. Heat Mass Transf.*, vol. 36, no. 4, pp. 365–371, April 2009. doi:10.1016/j.icheatmasstransfer.2009.01.006.

33. S.N. Sarada, A.V.S.R. Raju, K.K. Radha and L.S. Sunder, “Enhancement of heat transfer using varying width twisted tape inserts”, *Int. J. Eng. Sci. Technol.*, vol. 2, no. 6, pp. 107–118, 2010. https://www.ajol.info/index.php/ijest/article/view/63702/51529.

34. N. Piriyarungrod, S. Eiamsa-ard, C. Thianpong, M. Pimsam and K. Nanan, “Heat transfer enhancement by tapered twisted tape inserts”, *Chem. Engng. Processing: Process Intensification*, vol. 96, pp. 62–71, October 2015. doi:10.1016/j.cep.2015.08.002.

35. E. Esmaeilzadeh, H. Almohammadi, A. Nokhosteen, A. Motezaker and A.N. Omrani, “Study on heat transfer and friction factor characteristics of γ-Al2O3/water through circular tube with twisted tape inserts with different thicknesses”, *Int. J. Thermal Sci.*, vol. 82, pp. 72–83, August 2014. doi:10.1016/j.ijthermalsci.2014.03.005.

36. S. Eiamsa-ard and P. Promvonge, “Performance assessment in a heat exchanger tube with alternate clockwise and counter-clockwise twisted-tape inserts”, *Int. J. Heat Mass Transf.*, vol.53, no.7-8, pp.1364–1372, March 2010. doi:10.1016/j.ijheatmasstransfer.2009.12.023.

37. M.T. Naik, G.R. Janardana and L.S. Sundar, “Experimental investigation of heat transfer and friction factor with water-propylene glycol based CuO nanofluid in a tube with

twisted tape inserts", *Int. Comm. Heat Mass Transf.*, vol. 46, pp. 13-21, August 2013. doi:10.1016/j.icheatmasstransfer.2013.05.007.

38. K.A. Morteza and M. Eskandari, "Influence of twist length variations on thermal-hydraulic specifications of twisted-tape inserts in presence of Cu-water nanofluid", *Exp. Therm. Fluid Sci.*, vol. 61, pp. 230-240, Feb. 2015. doi:10.1016/j.expthermflusci.2014.11.004.

39. H. Maddah, M. Alizadeh, N. Ghasemi and S.R.W. Alwi, "Experimental study of Al2O3/water nanofluid turbulent heat transfer enhancement in the horizontal double pipes fitted with modified twisted tapes", *Int. J. Heat Mass Transf.*, vol. 78, pp. 1042-1054, November 2014. doi:10.1016/j.ijheatmasstransfer.2014.07.059.

40. S. Bhattacharyya and S.K. Saha, "Thermohydraulics of laminar flow through a circular tube having integral helical rib roughness and fitted with centre cleared twisted-tape", *Exp. Therm. Fluid Sci.*, vol. 42, pp. 154–162, Oct. 2012. doi:10.1016/j.expthermflusci.2012.05.002.

41. S. Bhattacharyya, S. Saha and S.K. Saha, "Laminar flow heat transfer enhancement in a circular tube having integral transverse rib roughness and fitted with centre cleared twisted-tape", *Exp. Therm. Fluid Sci.*,vol.44,pp.727–735,Jan.2013. doi:10.1016/j.expthermflusci.2012.09.016.

42. S.K. Saha, S. Bhattacharyya and P.K. Pal, "Thermohydraulics of laminar flow of viscous oil through a circular tube having integral axial rib roughness and fitted with centre-cleared twisted tape", *Exp. Therm. Fluid Sci*., vol. 41, pp. 121–129, September 2012. doi:10.1016/j.expthermflusci.2012.04.004.

43. S. Bhattacharyya, H. Chattopadhyay and A.C. Benim, "Simulation of heat transfer enhancement in tube flow with twisted tape insert", *Progress in Computational Fluid Dynamics*, vol. 17, no. 3, pp. 193-197, 2017. https://doi:10.1504/PCFD.2017.084356.

44. S. Bhattacharyya, H. Chattopadhyay, T.K. Pal and A. Roy, "Numerical investigation of thermohydraulics performance in elliptical twisted duct heat exchanger", in CAD/CAM,

robotics and factories of the future. Lecture Notes in Mechanical Engineering, D. K. Mandal and C. S. Syan, Eds. New Delhi, India: Springer, 2016, pp. 839-849.

45. C. Thianpong, P. Eiamsa-ard, K. Wongcharee and S. Eiamsa-ard, "Compound heat transfer enhancement of a dimpled tube with a twisted tape swirl generator", *Int. Comm. Heat MassTransf.*,vol.36,no.7,pp.698–704,Aug.2009.doi:10.1016/j.icheatmasstransfer.2009.03.026

46. H. Mengna, D. Xianhe, H. Kuo and L. Zhiwu, "Compound heat transfer enhancement of a converging–diverging tube with evenly spaced twisted-tapes", *Chinese J. Chem. Engng.*, vol. 15, no. 6, pp. 814–820, December 2007. doi:10.1016/S1004-9541(08)60008-7.

47. P. Sivashanmugam and S. Suresh, "Experimental studies on heat transfer and friction factor characteristics of laminar flow through a circular tube fitted with helical screw-tape inserts", *Appl. Therm. Eng.*, vol. 26, no. 16, pp. 1990–1997, November 2006. doi:10.1016/j.applthermaleng.2006.01.008.

48. M.S. El-Genk and T.M. Schriener, "A review and correlations for convection heat transfer and pressure losses in toroidal and helically coiled tubes", *Heat Transfer Engng.*, vol. 38, no. 5, pp. 447-474, October 2017. doi:10.1080/01457632.2016.1194693.

49. W. Wang, Y. Zhang, B. Li, Y. Li, Numerical investigation of tube-side fully developed turbulent flow and heat transfer in outward corrugated tubes, International Journal of Heat and Mass Transfer 116 (2018) 115-126.

50. H.A. Mohammed, A. K. Abbas, J.M. Sheriff, Influence of geometrical parameters and forced convective heat transfer in transversely corrugated circular tubes, International Communications in Heat and Mass Transfer 44 (2013) 116–126.

51. X. Tang, X. Dai, D. Zhu, Experimental and numerical investigation of convective heat transfer and fluid flow in twisted spiral tube, International Journal of Heat and Mass Transfer 90 (2015) 523–541.

52. S. Eiamsa-ard, S. Rattanawong, P. Promvonge, Turbulent convection in round tube equipped with propeller type swirl generators, International Communications in Heat and Mass Transfer 36 (2009) 357–364.

53. M.M.K. Bhuiya, M.S.U. Chowdhury, J.U. Ahamed, M.J.H. Khan, M.A.R. Sarkar, M.A. Kalam, H.H. Masjuki, M. Shahabuddin, Heat transfer performance for turbulent flow through a tube using double helical tape inserts, International Communications in Heat and Mass Transfer 39 (2012) 818–825.

54. P. Promvonge, Thermal performance in circular tube fitted with coiled square wires, Energy Conversion and Management 49 (2008) 980–987.

55. S. W. Chang, T. L. Yang, J. S. Liou, Heat transfer and pressure drop in tube with broken twisted tape insert, Experimental Thermal and Fluid Science 32 (2007) 489–501.

56. A. R. S. Suri, A. Kumar, R. Maithani, Experimental determination of enhancement of heat transfer in a multiple square perforated twisted tape inserts heat exchanger tube, Experimental Heat Transfer 31(5) (2018) 85-105.

57. A. Kumar, R. Kumar, R. Chauhan, M. Sethi, A. Kumari, N. Verma, R. Nadda, Single-phase thermal and hydraulic performance analysis of a V-pattern dimple obstacles air passage, Experimental Heat Transfer 30(5) (2017) 393-426.

Nomenclature

A tube inner wall surface area, m^2

b breadth of spring tape, m

c_p mean isobaric heat capacity, J/kgK

d corrugation height, m

D inner diameter of test tube, m

f Darcy friction factor

h convective heat transfer coefficient, W/m^2K

H winding pitch of spring, m

I current, A

k fluid thermal conductivity, W/mK

L tube length, m

m mass flow rate, kg/s

Nu Nusselt number

Δp pressure drop, N/m^2

P corrugation pitch of tube wall, m

Pr Prandtl number

R_w Wall thermal resistance, K/W

q_W Wall heat flux

Re Reynolds number based on D and V

s spring ratio

T temperature, K

V bulk velocity for plain tube (corrugation and spring tape free), m/s; voltage V

W width of spring tape, m

y pitch ratio

Greek Symbols

ρ fluid density, kg/m^3

Subscripts

b bulk

e electric

i inlet

o outlet

ow	outer wall
w	inner wall
0	plain tube (corrugation and spring tape free)